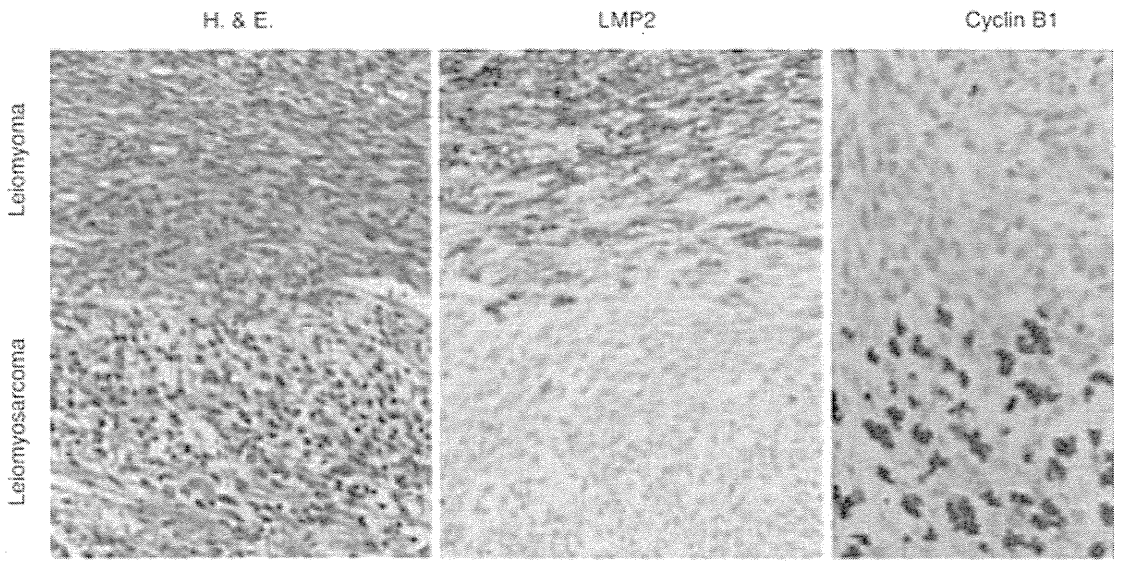

Figure 1 - Defect in LMP2/β1i expression and marked cyclin B1 expression in human uterine leiomyosarcoma tissue. Immunohistoc LMP2/β1i and cyclin B1 in human uterine leiomyoma and uterine leiomyosarcoma tissues located in the same tissue section. For 5-μm sections of tissue were stained with anti-LMP2/β1i and anti-cyclin B1 antibodies and protein expressions were revealed by conjugated anti-rabbit IgG antibody (×40 magnification). IHC experiments were performed with tissue sections from patient #1 leiomyoma and leiomyosarcoma are given in Table 3 and Table 4.

Ut-LMS mostly metastasizes to lung (around 25% of metastases), liver (65%) and other tissues (10%) by the hematological route, whereas metastases to small bowel, heart, brain and thyroid are rare[29]. Regional lymph node metastasis in patients with soft tissue sarcomas, except Ut-LMS, is an infrequent event occurring in around 2% of all patients[30-33]. The incidence of lymph node metastasis of Ut-LMS is uncertain and it is not known whether a sentinel lymph node biopsy is indicated in Ut-LMS. In our study, all lymph nodes were negative for Ut-LMS metastases, and IHC analyses showed positivity for cyclin B1 and ki-67 and negativity for LMP2/β1i. The histological findings were consistent with metastatic LMS for the skeletal muscle and rectum lesions. In WB experiments, cyclin B1 was expressed in Ut-LMS tissue sections from 5 patients (patients #1, #3, #6, #13 and #15), but not in leiomyoma tissue sections from the same 5 patients and normal myometrium sections from 2 patients (patients #1 and #3); these findings supported the IHC findings (Figure 2).

Although we previously demonstrated that abnormal expression of the ovarian steroid receptors, TP53 and ki-67 and mutations of TP53 were frequently associated with Ut-LMS, defective LMP2/β1i and calponin h1 expression and marked cyclin B1 expression appear to be more characteristic of Ut-LMS than these factors[27,34] (Figure 3, Table 3, Table 4). In further experiments, almost all leiomyomas showed staining for both ER and PR irrespective of the phase of the menstrual cycle, and the number of ki-67-positive cells was significantly lower in leiomyoma than Ut-LMS (Table 3, Table 4). IHC staining also demonstrated that almost all leiomyomas showed staining for TP53 (Table 4).

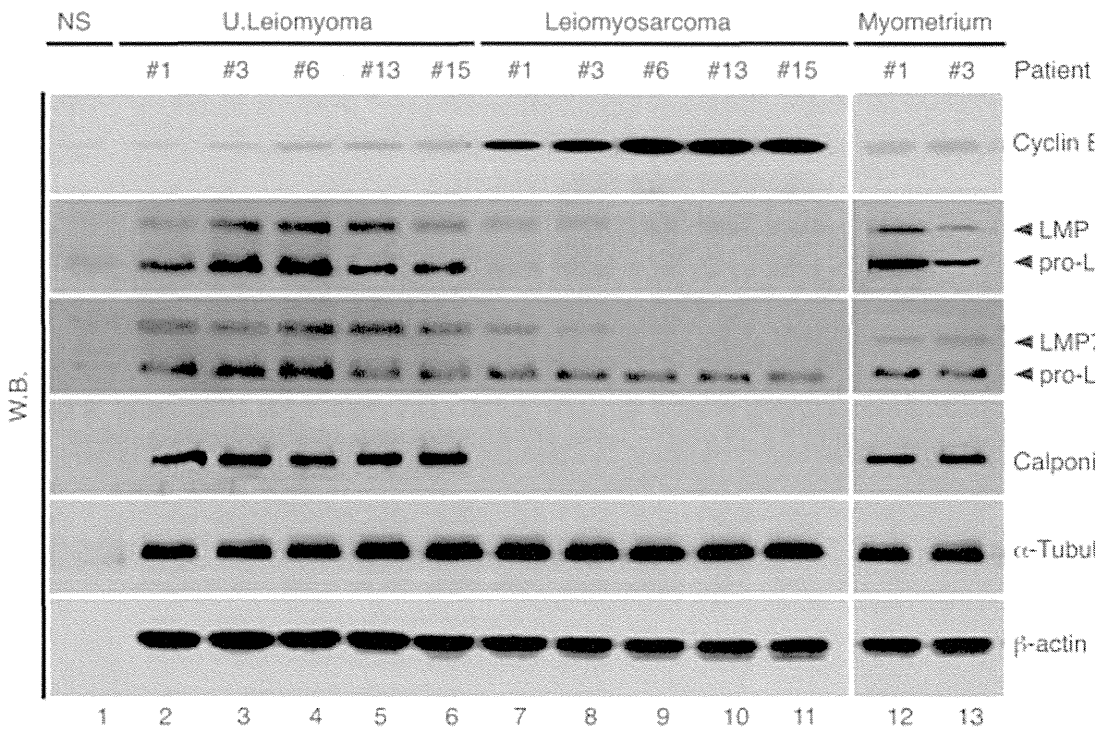

Figure 2 - Western blotting revealed cyclin B1, LMP2/β1i, LMP7/β5i, calponin h1, α-tubulin and β-actin in human uterine leiomyo leiomyosarcoma, and myometrium. Western blotting experiments were performed with tissue sections from 5 patients (patient #13, #15). Details of uterine leiomyoma and leiomyosarcoma are given in Table 3 and Table 4.

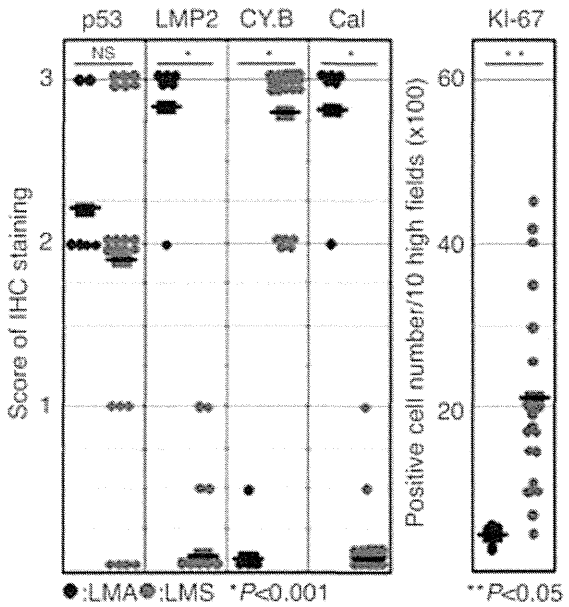

Figure 3 · Summary of IHC experiments for p53, LMP2, cyclin B, calponin h1 and ki-67 expression levels in leiomyoma (LMA) and leiomyosarcoma (LMS). IHC experiments were performed using 6 LMA tissue samples (patients #1, #3, #6, #13, #15, #21) and 22 LMS tissue samples (patients #1-#22) obtained from patients with LMA and/or LMS. The data are representative of 3 experiments.

Table 4 · Expression of ER, PR, Ki-67, LMP2/β1i, cyclin B1, calponin h1, and p53 in human leiomyoma

Patient	Age (years)	MC	Immunohistochemical staining						
			ER	PR	Ki-67	LMP2	Cy.B1	Calpo	p53
UL1	37	Luteal	+++	+++	31	+++	-	+++	++
UL3	45	Luteal	+++	+	38	+++	-	+++	++
UL6	49	Luteal	++	+++	28	++	-/+	+++	+++
UL13	51	Luteal	+++	++	34	+++	-	++	++
UL15	52	Luteal	++	++	39	+++	-	+++	+++
UL21	45	Luteal	++	++	29	+++	-	+++	++

MC, menstrual cycle; ER, estrogen receptor; PR, progesterone receptor; Ki-67, positive cell number/10 high-power fields; Cy.B1, cyclin B1; Calpo, calponin h1; UL, uterine leiomyoma.

Discussion

A recent report showed the expression of *LMP2/β1i* mRNA and protein in luminal and glandular epithelia, placenta villi, trophoblastic shells, and arterial endothelial cells[35]. These results implicate LMP2/β1i in the invasion of placental villi, degradation of the extracellular matrix, immune tolerance, glandular secretion, and angiogenesis[35]. Although the current studies help to elucidate the regulatory role of LMP2/β1i in the implantation of embryos, they do not contribute substantially to the knowledge of LMP2/β1i-mediated uterine sarcomagenesis. Cyclin B1, which is a regulatory protein involved in mitosis, forms a complex with Cdk1 to form the maturation-promoting factor (MPF)[36]. Cyclin B1 immunoreactivity was observed in the nucleus and the cytoplasm in all human Ut-LMS cases examined, but most cases of leiomyoma, bizarre leiomyoma and the normal myometrium were negative for cyclin B1. Cyclin B1/Cdk1 is involved in the early events of mitosis such as chromosome condensation, nuclear envelope breakdown, and spindle pole assembly. If cyclin B1 levels are depleted the cyclin B1/Cdk1 complex cannot form, cells cannot enter the M phase, and cell division slows down. Some anticancer therapies have been designed to prevent the cyclin B1/Cdk1 complex from forming in tumor cells to slow or prevent cell division [37]. Most of these methods have targeted the Cdk1 subunit, but there is an emerging interest in the oncology field to target cyclin B1 as well. That is, control of cyclin B1 may provide a clue to the development of a cure for human Ut-LMS. Clinical risk factors for development, however, have not been identified because of the absence of a suitable animal model. The LMP2/β1i-deficient mouse was the first animal model of spontaneous Ut-LMS to be established. Defective LMP2/β1i expression may be one of the causes of human Ut-LMS. To ascertain whether LMP2/β1i and cyclin B1 are potential biomarkers for distinguishing human Ut-LMS from other uterine mesenchymal tumors, we are investigating the reliability and characteristics of LMP2/β1i and cyclin B1 as diagnostic indicators with several clinical research facilities. The clinical research is yet to be concluded, and large-scale clinical studies need to be performed.

In conclusion, clarification of the correlation of LMP2/β1i and cyclin B1 with the development of human Ut-LMS and therefore the identification of specific risk factors may lead to the development of new treatments for the disease. Human Ut-LMS is refractory to chemotherapy and has a poor prognosis. The molecular biological and cytological information obtained from further research experiments with human tissues and LMP2/β1i-deficient mice will contribute to the development of preventive methods, a potential diagnostic biomarker, and new therapeutic approaches against human Ut-LMS.

References

1. Zaloudek C, Hendrickson MR: Mesenchymal tumors of the uterus. In: Blaustein's pathology of the female genital tract (5th edition), Kurman RJ (Ed), pp 561-578, Springer-Verlag, New York, 2002.
2. Gupta AA, Yao X, Verma S, Mackay H, Hopkins L; Sarcoma Disease Site Group and the Gynecology Cancer Disease Site Group: Systematic chemotherapy for inoperable, locally advanced, recurrent, or metastatic uterine leiomyosarcoma: a systematic review. Clin Oncol (R Coll Radiol), 25: 346-355, 2013.
3. Lin JF, Slomovitz BM: Uterine sarcoma. Curr Oncol Rep, 10: 512-518, 2008.
4. Amant F, Coosemans A, Debiec-Rychter M, Timmerman D, Vergote I: Clinical management of uterine sarcomas. Lancet Oncol, 10: 1188-1198, 2009.

5. National Institutes of Health: FACT SHEET-Uterine fibroids. Updated October 2010.
6. Chiang S, Oliva E: Recent developments in uterine mesenchymal neoplasms. Histopathol, 62: 124-137, 2013.
7. Kurma RJ: Pathology of the female genital tract, 4th ed, p 499, Springer-Verlag, New York, 2001.
8. Diagnostic criteria for leiomyosarcoma, adapted from 2003 WHO guidelines: World Health Organization Classification of Tumours: Pathology and genetics of tumours of the breast and female genital organs. IARC Press, Lyon, France, 2003.
9. Ravegnini G, Mariño-Enriquez A, Slater J, Eilers G, Wang Y, Zhu M, Nucci MR, George S, Angelini S, Raut CP, Fletcher JA: MED12 mutations in leiomyosarcoma and extrauterine leiomyoma. Mod Pathol, 26: 743-749, 2013.
10. Maniatis T: A ubiquitin ligase complex essential for the NF-kappaB, Wnt/Wingless, and Hedgehog signaling pathways. Genes Dev, 13: 505-510, 1999.
11. Shankaran V, Ikeda H, Bruce AT, White JM, Swanson PE, Old LJ, Schreiber RD: IFN-γ and lymphocytes prevent primary tumour development and shape tumour immunogenicity. Nature, 410: 1107-1111, 2001.
12. Van Kaer L, Ashton-Rickardt PG, Eichelberger M, Gaczynska M, Nagashima K, Rock KL, Goldberg AL, Doherty PC, Tonegawa S: Altered peptidase and viral-specific T cell response in LMP2 mutant mice. Immunity, 1: 533-541, 1994.
13. Hayashi T, Kodama S, Faustman DL: LMP2 expression and proteasome activity in NOD mice. Nat Med, 6: 1065-1066, 2000.
14. Hayashi T, Faustman DL: Development of spontaneous uterine tumors in low molecular mass polypeptide-2 knockout mice. Cancer Res, 62: 24-27, 2002.
15. Hayashi T, Kobayashi Y, Kohsaka S, Sano K: The mutation in the ATP-binding region of JAK1, identified in human uterine leiomyosarcomas, results in defective interferon-gamma inducibility of TAP1 and LMP2. Oncogene, 25: 4016-4026, 2006.
16. Nigg EA: Cyclin-dependent protein kinases: key regulators of the eukaryotic cell cycle. BioEssays, 17: 471-480, 1995.
17. Galderisi U, Jori FP, Giordano A: Cell cycle regulation and neural differentiation. Oncogene, 22: 5208-5219, 2003.
18. Orlando DA, Lin CY, Bernard A, Wang JY, Socolar JE, Iversen ES, Hartemink AJ, Haase SB: Global control of cell-cycle transcription by coupled CDK and network oscillators. Nature, 453: 944-947, 2008.
19. Ford HL, Pardee AB: Cancer and the cell cycle. J. Cell Biochem, Suppl 32-33: 166-172, 1999.
20. O'Connor DS, Wall NR, Porter AC, Altieri DC: A p34(cdc2) survival checkpoint in cancer. Cancer Cell, 2: 43-54, 2002.
21. Zhou XY, Wang X, Hu B, Guan J, Iliakis G, Wang Y: An ATM-independent S-phase checkpoint response involves CHK1 pathway. Cancer Res, 62: 1598-1603, 2002.
22. Agarwal R, Gonzalez-Angulo AM, Myhre S, Carey M, Lee JS, Overgaard J, Alsner J, Stemke-Hale K, Lluch A, Neve RM, Kuo WL, Sorlie T, Sahin A, Valero V, Keyomarsi K, Gray JW, Borresen-Dale AL, Mills GB, Hennessy BT: Integrative analysis of cyclin protein levels identifies cyclin b1 as a classifier and predictor of outcomes in breast cancer. Clin Cancer Res, 15: 3654-3662, 2009.
23. Hayashi T, Horiuchi A, Sano K, Hiraoka N, Kasai M, Ichimura T, Sudo T, Tagawa Y, Nishimura R, Ishiko O, Kanai Y, Yaegashi N, Aburatani H, Shiozawa T, Konishi I: Potential role of LMP2 as tumor-suppressor defines new targets for uterine leiomyosarcoma therapy. Sci Rep, 1: 180, 2011.
24. Hayashi T, Horiuchi A, Sano K, Hiraoka N, Kasai M, Ichimura T, Sudo T, Nishimura R, Ishiko O, Shiozawa T, Kanai Y, Yaegashi N, Aburatani H, Konishi I: Potential role of LMP2 as an anti-oncogenic factor in human uterine leiomyosarcoma: morphological significance of calponin h1. FEBS Lett, 586: 1824-1831, 2012.

25. Quade, BJ, Robboy, SJ: Uterine smooth muscle tumors. In: Robboy's pathology of the female reproductive tract, 2nd edition, Robboy SJ, Mutter GL, Prat J, Bentley RC, Russell P, Anderson MC, p 474, Churchill Livingstone Elsevier, Oxford, 2009.
26. Bell SW, Kempson RL, Hendrickson MR. Problematic uterine smooth muscle neoplasms. A clinicopathologic study of 213 cases. Am J Surg Pathol, 18: 535, 1994.
27. Zhai YL, Kobayashi Y, Mori A, Orii A, Nikaido T, Konishi I, Fujii S: Expression of steroid receptors, Ki-67, and p53 in uterine leiomyosarcomas. Int J Gynecol Pathol, 18: 20-28, 1999.
28. Komura D, Nishimura K, Ishikawa S, Panda B, Huang J, Nakamura H, Ihara S, Hirose M, Jones KW, Aburatani H: Noise reduction from genotyping microarrays using probe level information. In Silico Biol, 6: 79-92, 2006.
29. Echt G, Jepson J, Steel J, Langholz B, Luxton G, Hernandez W, Astrehan M, Petrovich Z: Treatment of uterine sarcomas. Cancer 66: 35-39, 1990.
30. Rose PG, Piver MS, Tsukada Y, Lau T: Patterns of metastasis in uterine sarcoma. Cancer, 63: 935-938, 1989.
31. Sondak VK, Chang AE: Clinical evaluation and treatment of soft tissue sarcomas. In: Enzinger and Weiss's soft tissue tumours, 4th edition, Weiss SW, Goldblum JR (Eds), pp 21-44, Mosby, St Louis, 2001.
32. Fong Y, Coit DG, Woodruff JM, Brennan MF: Lymph node metastasis from soft tissue sarcoma in adults: analysis of data from a prospective database of 1772 sarcoma patients. Ann Surg, 217: 72-77, 1993.
33. Behranwala KA, A'Hern R, Al-Muderis O, Thomas JM: Prognosis of lymph node metastasis in soft tissue sarcoma. Ann Surg Oncol, 11: 714-719, 2004.
34. Akhan SE, Yavuz E, Tecer A, Iyibozkurt CA, Topuz S, Tuzlali S, Bengisu E, Berkman S: The expression of Ki-67, p53, estrogen and progesterone receptors affecting survival in uterine leiomyosarcomas. A clinicopathologic study. Gynecol Oncol, 99: 36-42, 2005.
35. Wang HX, Wang HM, Li QL, Lin HY, Qian D, Zhu C: Expression of proteasome subunits low molecular mass polypeptide (LMP) 2 and LMP7 in the endometrium and placenta of rhesus monkey (macaca mulatta) during early pregnancy. Biol Reprod, 71: 1317-1324, 2004.
36. Moore JD, Kirk JA, Hunt T: Unmasking the S-phase-promoting potential of cyclin B1. Science, 300: 987-990, 2001.
37. Koliadi A, Nilsson C, Holmqvist M, Holmberg L, de La Torre M, Wärnberg F, Fjällskog ML: Cyclin B is an immunohistochemical proliferation marker which can predict for breast cancer death in low-risk node negative breast cancer. Acta Oncol, 49: 816-820, 2010.
38. Horiuchi A, Nikaido T, Ito K, Zhai Y, Orii A, Taniguchi S, Toki T, Fujii S: Reduced expression of calponin h1 in leiomyosarcoma of the uterus. Lab Invest, 78: 839-846, 1998.
39. Horiuchi A, Nikaido T, Taniguchi S, Fujii S: Possible role of calponin h1 as a tumor suppressor in human uterine leiomyosarcoma. J Natl Cancer Inst, 91: 790-796, 1999.

Laboratory Investigation (2014) 94, 683–691

Upregulated SMAD3 promotes epithelial–mesenchymal transition and predicts poor prognosis in pancreatic ductal adenocarcinoma

Ken Yamazaki[1], Yohei Masugi[1], Kathryn Effendi[1], Hanako Tsujikawa[1], Nobuyoshi Hiraoka[2], Minoru Kitago[3], Masahiro Shinoda[3], Osamu Itano[3], Minoru Tanabe[3], Yuko Kitagawa[3] and Michiie Sakamoto[1]

In pancreatic ductal adenocarcinoma (PDAC), features of epithelial–mesenchymal transition (EMT) are often seen in tumor tissue, and such features correlate with poor prognosis. Solitary infiltration of tumor cells represents a morphological phenotype of EMT, and we previously reported that a high degree of solitary cell infiltration correlates with EMT-like features, including reduced E-cadherin and elevated vimentin levels. Using solitary cell infiltration to evaluate the degree of EMT, gene-expression profiling of 12 PDAC xenografts was performed, and *SMAD3* was identified as an EMT-related gene. Immunohistochemistry using clinical specimens ($n = 113$) showed that SMAD3 accumulated in the nuclei of tumor cells, but was not detected in most epithelial cells in the pancreatic duct. Moreover, SMAD3 upregulation correlated with malignant characteristics, such as higher tumor grade and lymph node metastasis, as well as with EMT-like features. SMAD4, which plays a key role in transforming growth factor-β (TGF-β) signaling, is inactivated in approximately half of PDAC cases. In this study, the nuclear accumulation of SMAD3 was immunohistochemically detected even in SMAD4-negative cases. SMAD3 knockdown resulted in upregulated E-cadherin, downregulated vimentin, and reduced cell motility in pancreatic cancer cells regardless of SMAD4 status. In addition, TGF-β-treatment resulted in EMT induction in cells carrying wild-type *SMAD4*, and EMT was suppressed by SMAD3 knockdown. Patients with upregulated SMAD3 and a high degree of solitary cell infiltration had shorter times to recurrence and shorter survival times after surgery, and multivariate analysis showed that both factors were independent prognostic factors linked to unfavorable outcomes. These findings suggest that SMAD3 in PDAC is involved in the promotion of malignant potential through EMT induction in tumor cells regardless of SMAD4 status and serves as a potential biomarker of poor prognosis.
Laboratory Investigation (2014) **94,** 683–691; doi:10.1038/labinvest.2014.53; published online 7 April 2014

KEYWORDS: epithelial–mesenchymal transition; pancreatic ductal adenocarcinoma; prognosis; SMAD3; TGF-β

Pancreatic ductal adenocarcinoma (PDAC) is a leading cause of cancer death worldwide.[1] Despite recent advances in diagnosis and treatment, the prognosis of patients with PDAC is still extremely poor. Many pathologic features (eg, margin status, tumor size, tumor grade, and lymph node metastasis) have been shown to correlate with poor prognosis.[2–4] In addition, PDACs also often display the intratumoral heterogeneity of glandular differentiation. Among heterogeneous tumor cells, those capable of independently infiltrating into the stroma have the most dedifferentiated morphology and are frequently found at the invasion front. Moreover, we previously reported that an increase in the number of solitary infiltrating cells correlates with epithelial–mesenchymal transition (EMT)-like features, such as E-cadherin down-regulation and vimentin upregulation.[5]

EMT-like features are often seen in many types of cancer. Tumor cells with epithelial cell characteristics have apical–basal polarity and are organized in cell layers with cell–cell adhesion, whereas those with mesenchymal characteristics lose this polarity and migrate to the extracellular matrix. During EMT, tumor cells lose epithelial markers, such as E-cadherin and certain cytokeratins, and gain mesenchymal

[1]Department of Pathology, School of Medicine, Keio University, Tokyo, Japan; [2]Pathology Division, National Cancer Center Research Institute, Tokyo, Japan and [3]Department of Surgery, School of Medicine, Keio University, Tokyo, Japan
Correspondence: Professor M Sakamoto, MD, PhD, Department of Pathology, School of Medicine, Keio University, 35 Shinanomachi, Shunjuku-ku, Tokyo 160-8582, Japan.
E-mail: msakamot@z5.keio.jp

Received 29 October 2013; revised 10 February 2014; accepted 13 February 2014

markers such as vimentin and fibronectin.[6,7] Similarly, tumor cells in the standard cancer metastasis model dissociate from the tumor cell mass with tight cell–cell adhesion, invade the stroma, intravasate, circulate through the body, and form a secondary focus at a distant site. Thus, EMT can be considered an early event in cancer metastasis.

EMT is induced by extracellular signals including soluble factors, such as those in the transforming growth factor-β (TGF-β) super family, fibroblast growth factor families, and epidermal growth factor, as well as components of the extracellular matrix.[8] Overexpression of TGF-β in PDAC correlates with poor prognosis.[9] Interestingly, the *SMAD4* gene, which plays a key role in the TGF-β signaling pathway, is inactivated by mutations and deletions in 55% of PDAC cases.[10] Although TGF-β signaling seems to be abrogated by SMAD4 inactivation, nuclear accumulation of SMAD2 and SMAD3 has been found in SMAD4-null cells, indicating the presence of SMAD4-independent nuclear translocation of SMAD2 and SMAD3.[11] In PDAC, *SMAD4* mutations are associated with poor patient outcome.[10,12] Moreover, EMT-like features such as E-cadherin downregulation and an increased number of solitary infiltrating cells are also frequently found in PDACs, and such features correlate with poor prognosis.[5,13] These findings suggest that a SMAD4-independent signaling pathway could induce EMT-like features in PDAC.

Understanding the mechanism responsible for the induction of EMT in PDAC may contribute to improved diagnosis and treatment of patients. Previously, we showed that solitary cell infiltration serves as a morphological clue to EMT in PDAC.[5] In the current work, based on solitary cell infiltration as an indicator of EMT, we reanalyze gene expression profile of PDAC xenografts[14] in order to search for EMT-related genes and examine their role in PDAC.

MATERIALS AND METHODS

Clinical Specimens

PDAC tissues were obtained from patients who underwent surgical resection between 1995 and 2004 at Keio University Hospital ($n = 113$) and the National Cancer Center Hospital, Japan ($n = 12$).[14] All experiments using human samples were approved by the ethics committees of Keio University and the National Cancer Center. Tumor grade was evaluated according to the WHO tumor grading system.[15]

Microarray Analysis

Previously reported microarray data of 12 PDAC xenografts[14] were reanalyzed. Minimum information about a microarray experiment (MIAME)-compliant microarray data (experiment ID EXPR053) are accessible from our database, Genome Medicine Database of Japan (GeMDBJ; https://gemdbj.nibio.go.jp/dgdb/DownloadSite.do). Expression profiles were clustered using established algorithms implemented in the software program Cluster 2.0. Centroid linkage clustering with uncentered correlation was used, and TreeView software (http://rana.lbl.gov/EisenSoftware.htm) generated a visual representation of clusters.

Immunohistochemistry

Immunohistochemical staining using PDAC tissues from 113 patients was performed according to the method as previously described.[5] Rabbit polyclonal anti-SMAD3 antibody was obtained from Invitrogen (Carlsbad, CA, USA) and used in a 1:200 dilution. Sections were counterstained with hematoxylin. The medical records of all consecutive patients who underwent resection with curative intent for PDAC at Keio University Hospital were reviewed to examine the correlation with SMAD3 immunostaining.

In Vitro Analyses

Human PDAC cell lines AsPC-1, CFPAC-1, and PANC-1 were obtained from the American Type Culture Collection (Manassas, VA, USA). RNA interference (RNAi) was performed as previously described[14] using two siRNA molecules targeting the following sequences in SMAD3 mRNA: siSMAD3a, 5′-CCAGUGACCACCAGAUGAA-3′ and siSMAD3b, 5′-GGAGAAAUGGUGCGAGAAG-3′. These siRNAs and negative control siRNA were obtained from QIAGEN (Valencia, CA, USA). At 2 or 3 days after siRNA transfection, the transfectants were harvested for western blot and real-time RT-PCR analyses as previously described.[14,16] All primer sequences are shown in Supplementary Table 1.

At 24 h after transfection, cells were incubated with TGF-β (5 ng/ml; Sigma-Aldrich, St Louis, MO, USA) for 24 h and then harvested. Migration assays using Transwell inserts (Costar, Cambridge, MA, USA) were performed as previously described.[14] The number of migrated cells/field was determined by counting three fields from each transwell. Assays were performed in triplicate. Percent migration was defined as the ratio of the mean number of migrated SMAD3-knockdown cells to the mean number of migrated cells treated with negative control siRNA.

Statistical Analyses

Statistical analyses were performed using the Statistical Package for the Social Sciences (SPSS, Chicago, IL, USA), version 19.0, and P-values of <0.05 were considered statistically significant. Survival curves were calculated from the date of surgery using the Kaplan–Meier method and were compared using the log-rank test. Multivariate analyses were examined using the Cox proportional hazards regression model.

RESULTS

EMT Signature in PDACs

To identify EMT-related genes in PDAC, we reanalyzed gene expression profiles of xenografts derived from 12 PDAC patients[14] on the basis of the degree of solitary cell infiltration as an EMT-like feature. Previously, we showed that a high degree of solitary cell infiltration (SCI^{high}; seven or more solitary infiltrating tumor cells per 10 fields) significantly

correlates with EMT-like features including E-cadherin downregulation and vimentin upregulation.[5] Eight samples showed SCI^{high} and were classified as the high-EMT group (H1–H8), whereas four samples were classified as the low-EMT group (L1–L4) (Supplementary Table 2). Genes differentially expressed between the two groups were extracted based on the following criteria: mean signal (expression level) in one of the two groups is ≥ 1000 (when mean signal of all probe sets was normalized to 1000 in each microarray) and ≥ 2-fold that of the other group, with a *P*-value (Student's *t*-test) of ≤ 0.05. Figure 1a shows the result of two-way clustering analysis using 53 genes (66 probe sets) extracted as described above. The degree of solitary cell infiltration has been shown to correlate with vimentin upregulation and E-cadherin downregulation on immunohistochemical analyses;[5] however, these two genes did not satisfy the above differential expression criteria. This finding indicates that tumor cells showing such features were localized to the focal lesions, and their expression levels were not reflected in the tumor tissue as a whole.

One of the upregulated genes in the high-EMT group that met the differential expression criteria was the *SMAD3* gene. SMAD3 acts as a mediator of TGF-β signaling that is known to be involved in the EMT process. To confirm the differential SMAD3 expression levels between the two groups, immunohistochemistry was performed using the same tumor tissues that had been used for microarray analyses (H2, H4, L2, and L3 in Figure 1b). Increased positivity of SMAD3 in tumor cells was found in the high-EMT group compared with the low-EMT group. These results suggest that enhanced SMAD3 expression at the mRNA and protein levels may be related to EMT-like features in PDAC.

Upregulation of SMAD3 Correlates with PDAC Malignancy

To examine SMAD3 expression in clinical specimens, immunohistochemical analyses were performed using 113 cases of PDAC. Among these cases, the percentage of tumor cells with SMAD3-positive nuclear staining was highly heterogeneous (mean, 17.6%; median, 10%; range, 0–75%). SMAD3 was detected within the nucleus in almost all SMAD3-positive tumor cells, whereas nuclear accumulation of SMAD3 in epithelial cells of the pancreatic duct was rarely seen (Figure 2 and Supplementary Figure 1). These 113 cases were classified into two groups based on SMAD3 immunopositivity in the tumor cells ($SMAD3^{high}$, $\geq 15\%$ positivity; $SMAD3^{low}$, $<15\%$), and SMAD3 status was compared with clinicopathological parameters (Table 1). $SMAD3^{high}$ correlated with larger tumor size, major vessel involvement, higher tumor grade, and lymph node metastasis. Furthermore, $SMAD3^{high}$ also correlated with reduced E-cadherin and elevated vimentin levels as well as a high degree of solitary cell infiltration (Table 1). SMAD4 was detected in 41% of PDAC cases; however, no correlation was observed between the immunostaining status of SMAD3 and

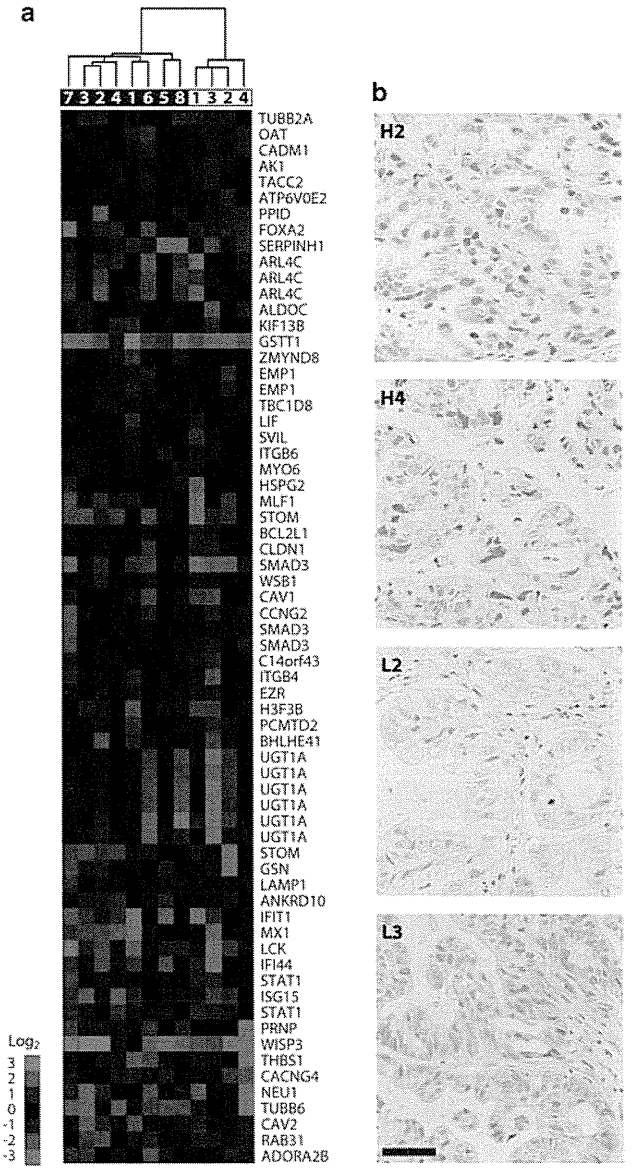

Figure 1 Two-dimensional clustering analysis of the genes differentially expressed between high- and low-EMT groups. (**a**) The vertical and horizontal axes of the heat map represent genes and tumor samples, respectively. White numbers indicate sample numbers of the high-EMT group (H1 – H8), and black numbers indicate the low-EMT group (L1–L4). Gene expression levels are represented by the $\log_2$ mean intensity ratio and depicted in terms of color variation from red (high expression) to blue (low expression). (**b**) Expression of SMAD3 was confirmed by immunohistochemistry using tumor tissues (H2, H4, L2, and L3). Scale bar = 100 μm.

SMAD4 ($P = 0.146$). In SMAD4-negative cases, nuclear accumulation of SMAD3 with reduced E-cadherin expression was frequently observed at the invasion front of tumor cells (Figure 2 and Supplementary Figure 1).

SMAD3 Knockdown Reduces EMT-Like Features

SMAD3 expression levels were examined in representative PDAC cell lines. Compared with other gastrointestinal cancer

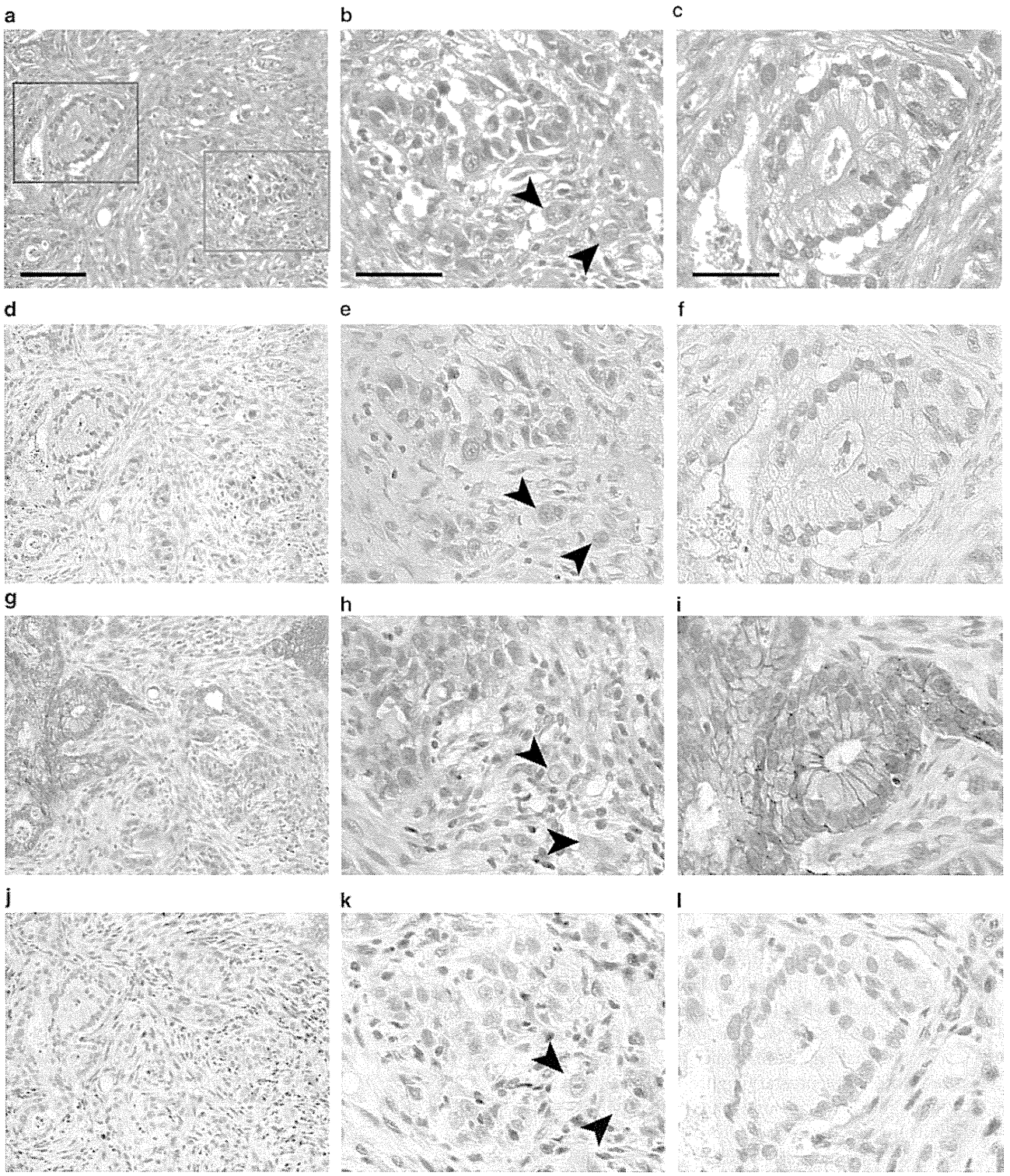

Figure 2 Immunohistochemical detection of SMAD3, E-cadherin, and SMAD4. Serial sections derived from formalin-fixed, paraffin-embedded pancreatic cancer tissue were stained with H&E (**a**–**c**) or DAB followed by probing with anti-SMAD3 (**d**–**f**), anti-E-cadherin (**g**–**i**), and anti-SMAD4 (**j**–**l**) antibodies. Solitary infiltrating cells were frequently observed (arrowheads) at the invasive front (red box in **a**; **b**, **e**, **h**, **k**, high-power fields) compared with the tumor center (blue box in **a**; **c**, **f**, **i**, **l**, high-power fields). Lymphocytes and stromal cells showed SMAD4-positive nuclei. Scale bars represent 100 μm (**a**) and 50 μm (**b**, **c**).

Table 1 Correlation between clinicopathological characteristics and SMAD3 immunolabeling

Characteristics	SMAD3-positive rate <15%	SMAD3-positive rate ≥15%	χ^2 test *P*-value
Mean age (years old)	64.8	65.3	0.786[a]
Gender			0.901
Female	21	20	
Male	36	36	
Mean tumor size (cm)	2.64	3.23	0.005[a]
Tumor location			0.457
Pancreatic head	37	40	
Pancreatic body/tail	20	16	
Large vessel involvement			0.025
Negative	43	31	
Positive	14	25	
Neural invasion			0.212[b]
Negative	5	1	
Positive	52	55	
Lymph node metastasis			<0.001
Negative	20	3	
Positive	37	53	
Margin status			0.788
Negative	42	40	
Positive	15	16	
Tumor grade			<0.001
1–2	52	32	
3	5	24	
SMAD4 status			0.146
Negative	30	37	
Positive	27	19	
E-cadherin status			0.028
Preserved	30	18	
Reduced	27	38	
Vimentin status			0.002
Not expressed	43	26	
Expressed	14	30	
Degree of solitary cell infiltration			<0.001
Low	26	8	
High	31	48	

[a]Student's *t*-test.
[b]Fisher's exact test.

cell lines, PDAC cell lines commonly showed higher SMAD3 mRNA levels (Supplementary Figure 2). The AsPC-1, CFPAC-1, and PANC-1 cell lines were then selected for further *in vitro* analyses. Although SMAD4 is inactivated in AsPC-1 and CFPAC-1 cells,[17,18] SMAD3 expression was detected in the nuclei of these cells, as well as in PANC-1 cells that carry the wild-type *SMAD4* allele (Supplementary Figure 3). TGF-β induced morphological change and growth arrest in PANC-1 cells, whereas no responses were observed in SMAD4-inactivated cells (Supplementary Figures 4 and 5).

Treatment of these three cell lines with siRNA molecules targeting SMAD3 resulted in decreased SMAD3 expression at both the mRNA and protein levels (Figure 3 and Supplementary Figure 6). In PANC-1 cells, TGF-β treatment induced EMT features as shown by *E-cadherin* down-regulation and *vimentin* upregulation (compare control + TGF-β with control − TGF-β in Figure 3b); however, SMAD3 knockdown suppressed these EMT features (compare siSMAD3 + TGF-β with control + TGF-β). SMAD3 knockdown also suppressed TGF-β-induced morphological change and *CDKN1A (p21)* upregulation in PANC-1 cells (Supplementary Figure 6). These results suggest that TGF-β-induced EMT is a SMAD3- and SMAD4-dependent process. In SMAD4-inactivated AsPC-1 and CFPAC-1 cells, SMAD3 knockdown resulted in increased *E-cadherin* and reduced *vimentin* gene expression (compare siSMAD3 − TGF-β with control − TGF-β), suggesting that SMAD3 is involved in SMAD4-independent EMT and that TGF-β is not required for SMAD4-independent, SMAD3-induced EMT at least in these two cell lines. After SMAD3 knockdown, AsPC-1 cells formed larger cell clusters with decreased cell scattering, whereas CFPAC-1 and PANC-1 cells showed reduced lamellipodial protrusions compared with controls (Figure 3c). To examine whether these morphological changes could contribute to reduced cell motility, migration assays were performed. SMAD3 knockdown decreased the number of cells that migrated through Transwell inserts in all cell lines (Figure 3d).

SMAD3^{high} Correlates with Poor Prognosis

Univariate analysis showed that, in addition to SMAD3^{high}, EMT-like features such as reduced E-cadherin, elevated vimentin, and SCI^{high} correlated with shorter survival times

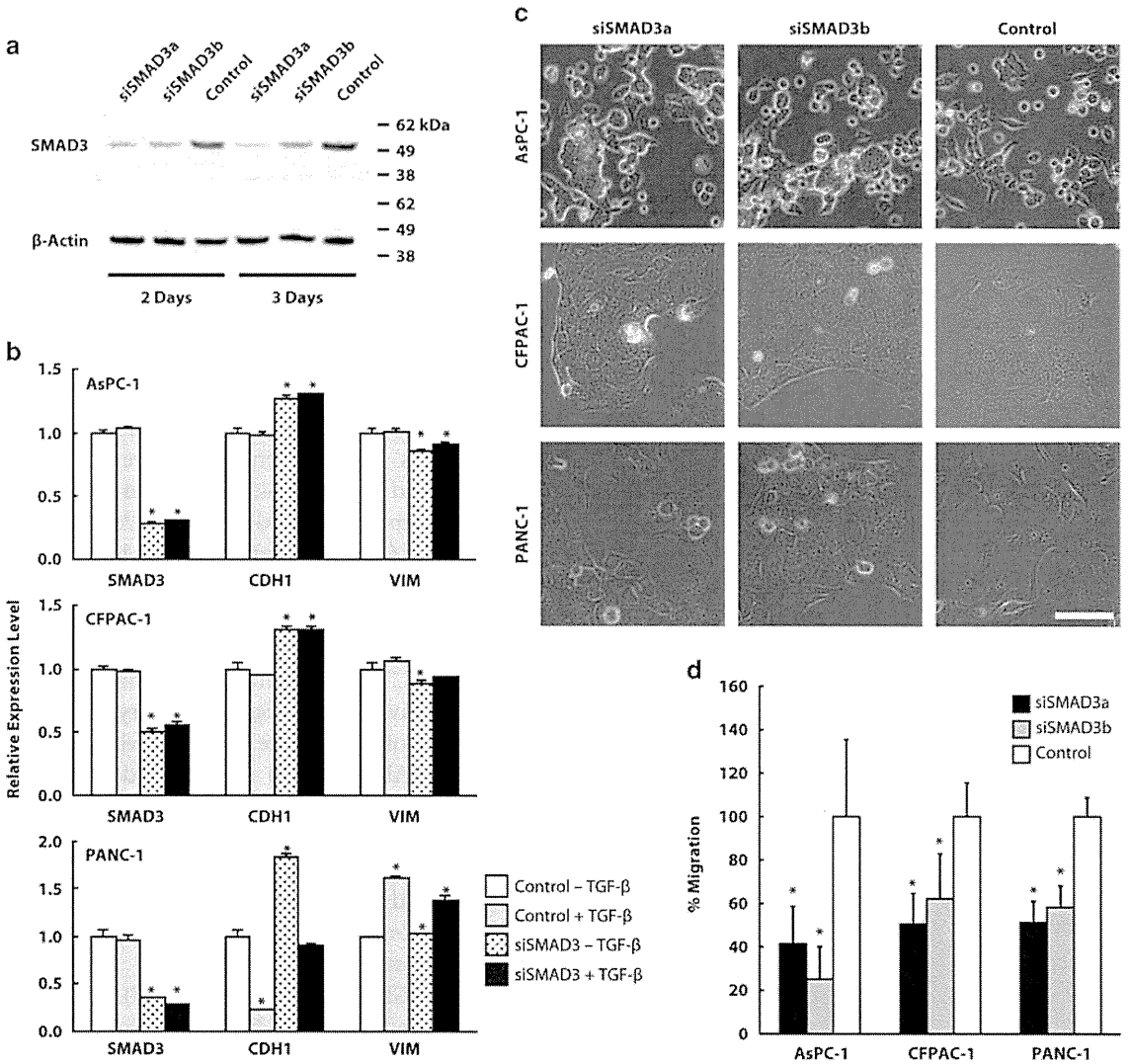

Figure 3 SMAD3 knockdown arrested the induction of EMT. (**a**) Western blots showed that two siRNA molecules targeting SMAD3 (siSMAD3a and siSMAD3b) were effective at reducing SMAD3 protein levels in AsPC-1 cells at 2 and 3 days after siRNA transfection. (**b**) AsPC-1, CFPAC-1, and PANC-1 cells were transfected with siSMAD3a or control siRNA and then treated with 5 ng/ml TGF-β for 24 h. Expression levels of *SMAD3*, *E-cadherin (CDH1)*, and *vimentin (VIM)* in these cells were examined by quantitative RT-PCR. The expression levels were normalized to those of *GAPDH* in each cell line. The relative expression level shows the ratio of mRNA levels in siSMAD3a transfectants compared with the control cells without TGF-β treatment (white bars). (**c**) SMAD3 knockdown resulted in morphological changes in AsPC-1, CFPAC-1, and PANC-1 cells. Scale bar = 100 μm. (**d**) Transwell migration assays showed a reduced number of migrated transfectants after SMAD3 knockdown compared with control cells. Error bars indicate the s.d. of the ratio of migrated cells/field (mean number of migrated cells in each control = 100%) of experiments carried out in triplicate. Asterisks indicate a *P*-value of <0.05 compared with controls.

(Table 2). SMAD3 and solitary cell infiltration were identified as independent prognostic factors by multivariate analysis. Kaplan–Meier analyses showed that SMAD3^{high} was associated with shorter overall survival (Figure 4a) and also with early recurrence (Figure 4c). Moreover, patients with both SMAD3^{high} and SCI^{high} had a less favorable prognosis than others (Figures 4b and d). On the other hand, SMAD4 status was not associated with poor prognosis in this study (Supplementary Figure 7), whereas SMAD4 positivity correlated with EMT-like features in SMAD3^{high} cases (Supplementary Table 3).

DISCUSSION

TGF-β signaling is known to play a dual role in the regulation of proliferative and invasive properties of cancer.[19,20] TGF-β can induce EMT in PDAC cells,[21,22] and overexpression of TGF-β in PDAC correlates with decreased survival.[9] In many gastrointestinal cancers, responses to TGF-β are decreased by mutations or loss of expression of TGF-β receptors and SMADs.[23] Inactivation of SMAD4 through genetic aberrations occurs frequently in pancreatic and colorectal cancers. Although *SMAD4* mutations are rare in gastric cancer, SMAD4 inactivation at the protein level is involved in

Table 2 Univariate and multivariate analyses of EMT-like features associated with overall survival

	Univariate		Multivariate	
EMT-like features	HR (95% CI)	*P*-value	HR (95% CI)	*P*-value
SMAD3				
Low *vs* high	2.829 (1.628–4.918)	<0.001	1.843 (1.006–3.377)	0.048
E-cadherin				
Reduced *vs* preserved	0.529 (0.304–0.922)	0.025	0.875 (0.475–1.612)	0.875
Vimentin				
Not expressed *vs* expressed	2.833 (1.637–4.926)	<0.001	1.795 (0.971–3.317)	0.062
Degree of solitary infiltrating cells				
Low *vs* high	3.214 (1.604–6.440)	0.001	2.177 (1.038–4.565)	0.040

Abbreviations: CI, confidence interval; HR, hazard ratio.

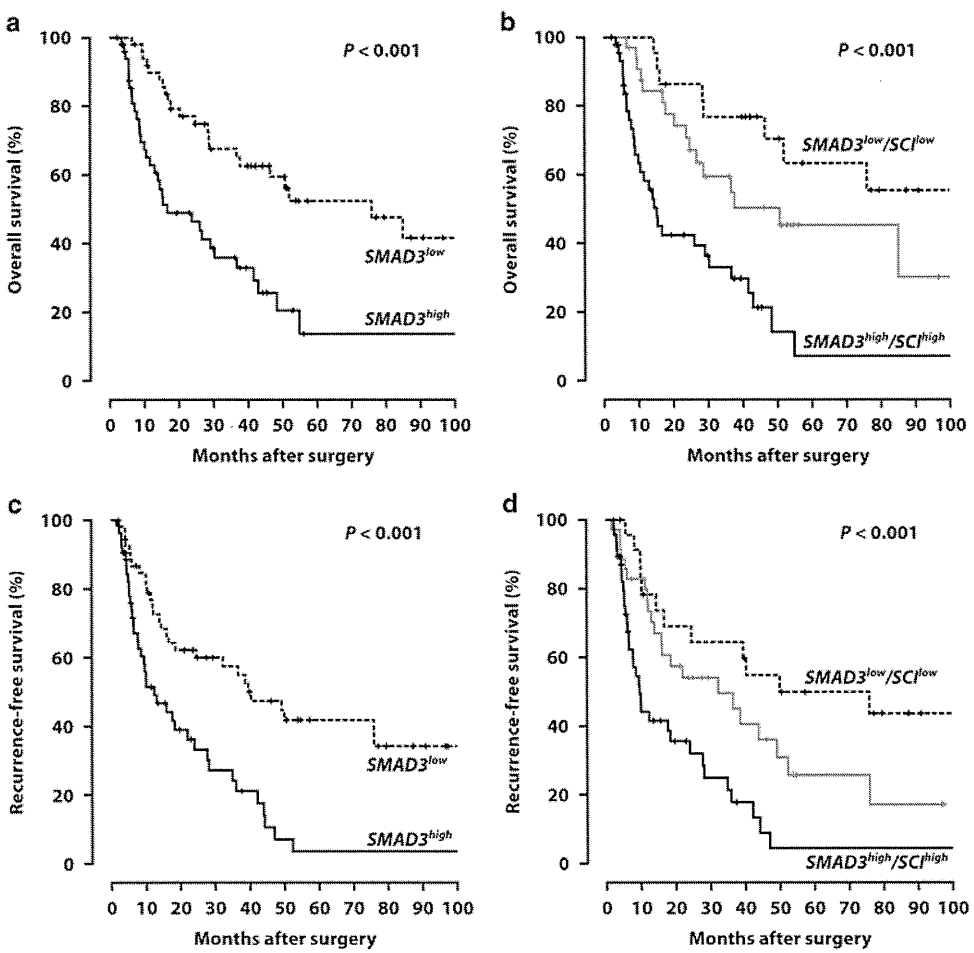

Figure 4 Kaplan–Meier survival analyses. Overall survival (**a**, **b**) and recurrence-free survival (**c**, **d**) were compared among patients with $SMAD3^{low}$ and $SMAD3^{high}$ (**a**, **c**), or $SMAD3^{low}/SCI^{low}$, $SMAD3^{high}/SCI^{high}$, and others (gray lines) (**b**, **d**). The *P*-value of the log-rank test for each analysis is indicated.

gastric cancer progression.[24] In our study, 67/113 cases (59%) were SMAD4 negative. As immunohistochemical labeling for SMAD4 mirrors genetic status,[25] SMAD4 was most likely inactivated in the SMAD4-negative cases.

TGF-β-induced EMT has been thought of as a SMAD4-dependent process. Here, we show that EMT-like features, such as reduced E-cadherin, elevated vimentin, and increased cell motility, were not induced in SMAD4-inactivated AsPC-1 and CFPAC-1 cells by TGF-β treatment, whereas TGF-β treatment significantly induced EMT-like features in SMAD4-positive PANC-1 cells. These findings are in agreement with a previous report from Ellenrieder *et al.*[21] However, some researchers have reported that TGF-β-induced EMT can also occur in a SMAD4-independent manner.[26,27] TGF-β can induce the activation of the mitogen-activated protein kinase (MAPK) signaling pathway that is involved in EMT induction independently of the canonical TGF-β signaling pathway.[26] Levy *et al*[27] also showed that TGF-β-induced EMT is independent of SMAD4 and suggested that SMAD4-independent noncanonical TGF-β signaling pathway or other pathways may be involved in EMT induction. Thus, the mechanism involved in TGF-β-induced EMT is still controversial.

Interestingly, we observed that SMAD3 knockdown in the cells without TGF-β treatment also resulted in suppression of EMT-like features. Therefore, to induce EMT, SMAD3 may be involved in another pathway in addition to the canonical TGF-β signaling pathway. Zhao *et al*[28] reported that signal transducer and activator of transcription 3 (STAT3) is activated in SMAD4-inactivated PDACs and suggested that loss of SMAD4, leading to aberrant activation of STAT3, contributes to the switch of TGF-β from a tumor-suppressive to a tumor-promoting pathway. As SMAD3 upregulation correlated with EMT-like features in PDACs regardless of SMAD4 status, it remains unclear whether SMAD3 cooperates with STAT3 to induce EMT in SMAD4-inactivated cases.

Here, we examined gene expression profiles of PDACs on the basis of solitary cell infiltration to identify other EMT-related genes that may increase the malignant potential of PDAC. These gene expression profiles revealed that enhanced expression of the *SMAD3* gene was associated with EMT in PDAC. Immunohistochemical analysis confirmed that SMAD3 expression was mostly undetectable in nonneoplastic epithelia of the pancreas, but was readily apparent in the nuclei of tumor cells, despite the heterogeneous positivity observed among our cases. SMAD3 expression levels in PDAC cells were commonly high compared with other gastrointestinal (colon and stomach) cancer cells. SMAD3 overexpression correlates with Gleason score and expression of proliferating cell nuclear antigen in prostate cancer.[29] Here, we found that high SMAD3 immunopositivity correlated with larger tumor size, major vessel involvement, higher tumor grade, and lymph node metastasis, all of which are characteristics associated with a poor prognosis in PDAC patients.[2–4] Moreover, SMAD3^{high} patients had a shorter survival time after surgery than SMAD3^{low} patients. These results suggest that enhanced SMAD3 expression may facilitate the malignant progression of PDAC.

EMT-like features in PDAC have been implicated as biomarkers for poor prognosis.[5,13,30] Here, we showed that high SMAD3 immunopositivity was associated with vascular invasion and lymph node metastasis as well as EMT-like features, suggesting that SMAD3-mediated EMT may promote invasion and metastasis, thereby linking it to poor prognosis. Besides SMAD3^{high}, we also identified SCI^{high} as another independent predictor of poor prognosis. The group of patients with both SMAD3^{high} and SCI^{high} had the least favorable prognosis compared with other groups. *In vitro* analysis revealed that SMAD3 knockdown resulted in reduced cell motility, suggesting that SMAD3 may be involved in cell migration. In 113 cases of PDAC, SMAD3^{high} significantly correlated with SCI^{high}, and both were found to be independent factors for poor prognosis. Although it is clear that SMAD3 is involved in the malignancy process, most likely by inducing EMT, it is possible that the malignancy process is mediated by SMAD3 via another mechanism as well. EMT has been shown to result in cancer cells with stem cell-like characteristics that have a propensity to invade surrounding tissue and display resistance to certain therapies.[31] Sun *et al*[32] showed that NANOG promotes liver cancer cell invasion by inducing EMT through NODAL/SMAD3 signaling pathway. In human embryonic stem cells, SMAD2 and SMAD3 are involved in the transcriptional regulation of *OCT4* and *NANOG*[33] and control of the balance between self-renewal and differentiation.[34] These findings may provide clues to clarify a possible mechanism underlying the malignant process of PDACs mediated by SMAD3.

In conclusion, enhanced expression of SMAD3 in PDAC correlated with malignant characteristics including EMT-like features, lymph node metastasis, and poor prognosis. SMAD3 seems to play an important role in malignant progression through EMT induction in PDAC, and may provide a potential biomarker for poor prognosis of PDAC.

Supplementary Information accompanies the paper on the Laboratory Investigation website (http://www.laboratoryinvestigation.org)

ACKNOWLEDGMENTS

This study was supported by grants from The New Energy and Industrial Technology Development Organization (Project no. P10003) and from The Ministry of Health, Labour and Welfare of Japan (Grant-in-aid of The Third Term Comprehensive 10-Year Strategy for Cancer Control).

DISCLOSURE/CONFLICT OF INTEREST

The authors declare no conflict of interest.

1. Jemal A, Bray F, Center MM, *et al.* Global cancer statistics. CA Cancer J Clin 2011;61:69–90.

2. Trede M, Schwall G, Saeger HD. Survival after pancreatoduodenectomy. 118 consecutive resections without an operative mortality. Ann Surg 1990;211:447–458.
3. Yeo CJ, Cameron JL, Lillemoe KD, *et al.* Pancreaticoduodenectomy for cancer of the head of the pancreas. 201 patients. Ann Surg 1995;221:721–731.
4. Lüttges J, Schemm S, Vogel I, *et al.* The grade of pancreatic ductal carcinoma is an independent prognostic factor and is superior to the immunohistochemical assessment of proliferation. J Pathol 2000;191: 154–161.
5. Masugi Y, Yamazaki K, Hibi T, *et al.* Solitary cell infiltration is a novel indicator of poor prognosis and epithelial-mesenchymal transition in pancreatic cancer. Hum Pathol 2010;41:1061–1068.
6. Thiery JP. Epithelial-mesenchymal transitions in tumor progression. Nat Rev Cancer 2002;2:442–454.
7. Thiery JP, Acloque H, Huang RYJ, *et al.* Epithelial-mesenchymal transitions in development and disease. Cell 2009;139:871–890.
8. Thiery JP, Sleeman JP. Complex networks orchestrate epithelial-mesenchymal transitions. Nat Rev Mol Cell Biol 2006;7:131–142.
9. Friess H, Yamanaka Y, Büchler M, *et al.* Enhanced expression of transforming growth factor beta isoforms in pancreatic cancer correlates with decreased survival. Gastroenterology 1993;105:1846–1856.
10. Tascilar M, Skinner HG, Rosty C, *et al.* The SMAD4 protein and prognosis of pancreatic ductal adenocarcinoma. Clin Cancer Res 2001;7:4115–4121.
11. Fink SP, Mikkola D, Willson JKV, *et al.* TGF-beta-induced nuclear localization of Smad2 and Smad3 in Smad4 null cancer cell lines. Oncogene 2003;22:1317–1323.
12. Blackford A, Serrano OK, Wolfgang CL, *et al.* SMAD4 gene mutations are associated with poor prognosis in pancreatic cancer. Clin Cancer Res 2009;15:4674–4679.
13. Shimamura T, Sakamoto M, Ino Y, *et al.* Dysadherin overexpression in pancreatic ductal adenocarcinoma reflects tumor aggressiveness: relationship to e-cadherin expression. J Clin Oncol 2003;21:659–667.
14. Yamazaki K, Takamura M, Masugi Y, *et al.* Adenylate cyclase-associated protein 1 overexpressed in pancreatic cancers is involved in cancer cell motility. Lab Invest 2009;89:425–432.
15. Hruban RH, Boffetta P, Hiraoka N, *et al.* Tumors of the pancreas. In: Bosman FT, Carneiro F, Hruban RH, *et al.* (eds). World Health Organization Classification of Tumors of the Digestive System, Lyon, France, 2010, pp 279–337.
16. Uchida H, Yamazaki K, Fukuma M, *et al.* Overexpression of leucine-rich repeat-containing G protein-coupled receptor 5 in colorectal cancer. Cancer Sci 2010;101:1731–1737.
17. Schutte M, Hruban RH, Hedrick L, *et al.* DPC4 gene in various tumor types. Cancer Res 1996;56:2527–2530.
18. Moore PS, Sipos B, Orlandini S, *et al.* Genetic profile of 22 pancreatic carcinoma cell lines. Analysis of K-ras, p53, p16 and DPC4/Smad4. Virchows Arch 2001;439:798–802.
19. Welch DR, Fabra A, Nakajima M. Transforming growth factor beta stimulates mammary adenocarcinoma cell invasion and metastatic potential. Proc Natl Acad Sci USA 1990;87:7678–7682.
20. Markowitz SD, Roberts AB. Tumor suppressor activity of the TGF-beta pathway in human cancers. Cytokine Growth Factor Rev 1996;7: 93–102.
21. Ellenrieder V, Hendler SF, Boeck W, *et al.* Transforming growth factor beta1 treatment leads to an epithelial-mesenchymal transdifferentiation of pancreatic cancer cells requiring extracellular signal-regulated kinase 2 activation. Cancer Res 2001;61:4222–4228.
22. Jungert K, Buck A, Buchholz M, *et al.* Smad-Sp1 complexes mediate TGFbeta-induced early transcription of oncogenic Smad7 in pancreatic cancer cells. Carcinogenesis 2006;27:2392–23401.
23. Achyut BR, Yang L. Transforming growth factor-β in the gastrointestinal and hepatic tumor microenvironment. Gastroenterology 2011;141:1167–1178.
24. Wang L, Kim S, Lee JH, *et al.* Inactivation of SMAD4 tumor suppressor gene during gastric carcinoma progression. Clin Cancer Res 2007;13: 102–110.
25. Wilentz RE, Su GH, Dai JL, *et al.* Immunohistochemical labeling for dpc4 mirrors genetic status in pancreatic adenocarcinomas: a new marker of DPC4 inactivation. Am J Pathol 2000;156:37–43.
26. Giehl K, Imamichi Y, Menke A. Smad4-independent TGF-beta signaling in tumor cell migration. Cells Tissues Organs 2007;185: 123–130.
27. Levy L, Hill CS. Smad4 dependency defines two classes of transforming growth factor β (TGF-β) target genes and distinguishes TGF-β-induced epithelial-mesenchymal transition from its antiproliferative and migratory responses. Mol Cell Biol 2005;25:8108–8125.
28. Zhao S, Venkatasubbarao K, Lazor JW, *et al.* Inhibition of STAT3 Tyr705 phosphorylation by Smad4 suppresses transforming growth factor β-mediated invasion and metastasis in pancreatic cancer cells. Cancer Res 2008;68:4221–4228.
29. Lu S, Lee J, Revelo M, *et al.* Smad3 is overexpressed in advanced human prostate cancer and necessary for progressive growth of prostate cancer cells in nude mice. Clin Cancer Res 2007;13: 5692–5702.
30. Javle MM, Gibbs JF, Iwata KK, *et al.* Epithelial-mesenchymal transition (EMT) and activated extracellular signal-regulated kinase (p-Erk) in surgically resected pancreatic cancer. Ann Surg Oncol 2007;14: 3527–3533.
31. Polyak K, Weinberg RA. Transitions between epithelial and mesenchymal states: acquisition of malignant and stem cell traits. Nat Rev Cancer 2009;9:265–273.
32. Sun C, Sun L, Jiang K, *et al.* NANOG promotes liver cancer cell invasion by inducing epithelial-mesenchymal transition through NODAL/SMAD3 signaling pathway. Int J Biochem Cell Biol 2013;45:1099–1108.
33. Brown S, Teo A, Pauklin S, *et al.* Activin/Nodal signaling controls divergent transcriptional networks in human embryonic stem cells and in endoderm progenitors. Stem Cells 2011;29:1176–1185.
34. Singh AM, Reynolds D, Cliff T, *et al.* Signaling network crosstalk in human pluripotent cells: a Smad2/3-regulated switch that controls the balance between self-renewal and differentiation. Cell Stem Cell 2012;10:312–326.

Cancer Medicine

Open Access

ORIGINAL RESEARCH

Copy number increase of *ACTN4* is a prognostic indicator in salivary gland carcinoma

Yukio Watabe[1,2], Taisuke Mori[3], Seiichi Yoshimoto[4], Takeshi Nomura[2], Takahiko Shibahara[2], Tesshi Yamada[1] & Kazufumi Honda[1]

[1]Division of Chemotherapy and Clinical Research, National Cancer Center Research Institute, Tokyo 104-0045, Japan
[2]Department of Oral and Maxillofacial Surgery, Tokyo Dental College, Chiba 261-8502, Japan
[3]Division of Molecular Pathology, National Cancer Center Research Institute, Tokyo 104-0045, Japan
[4]Department of Head and Neck Oncology, National Cancer Center Hospital, Tokyo 104-0045, Japan

Keywords
Actinin-4, *ACTN4*, head and neck cancer, prognostic marker, salivary gland carcinoma

Correspondence
Kazufumi Honda, Division of Chemotherapy and Clinical Research, National Cancer Center Research Institute, 5-1-1 Tsukiji, Chuo-ku, Tokyo 104-0045, Japan.
Tel: +81-3-3542-2511; Fax: +81-3-3547-6045;
E-mail: khonda@ncc.go.jp

Funding Information
This work was supported by a Grant-in Aid for Scientific Research (B) and a Challenging Exploratory Research from the Ministry of Education, Culture, Sports, Science and Technology (METX) of Japan (K. H.), and the National Cancer Center Research and Development Fund (23-A-38, and 23-A-11) (K. H.).

Received: 10 December 2013; Revised: 23 January 2014; Accepted: 28 January 2014

***Cancer Medicine* 2014; 3(3): 613–622**

doi: 10.1002/cam4.214

Abstract

Copy number increase (CNI) of *ACTN4* has been associated with poor prognosis and metastatic phenotypes in various human carcinomas. To identify a novel prognostic factor for salivary gland carcinoma, we investigated the copy number of *ACTN4*. We evaluated DNA copy number of *ACTN4* in 58 patients with salivary gland carcinoma by using fluorescent in situ hybridization (FISH). CNI of *ACTN4* was recognized in 14 of 58 patients (24.1%) with salivary gland carcinoma. The cases with CNI of *ACTN4* were closely associated with histological grade ($P = 0.047$) and vascular invasion ($P = 0.033$). The patients with CNI of *ACTN4* had a significantly worse prognosis than the patients with normal copy number of *ACTN4* ($P = 0.0005$ log-rank test). Univariate analysis by the Cox proportional hazards model showed that histological grade, vascular invasion, and CNI of *ACTN4* were independent risk factors for cancer death. Vascular invasion (hazard ratio [HR]: 7.46; 95% confidence interval [CI]: 1.98–28.06) and CNI of *ACTN4* (HR: 3.23; 95% CI: 1.08–9.68) remained as risk factors for cancer death in multivariate analysis. Thus, CNI of *ACTN4* is a novel indicator for an unfavorable outcome in patients with salivary gland carcinoma.

Introduction

Salivary gland carcinomas are rare malignant tumors comprising about 5% of cancers of the head and neck region [1]. In addition, the histopathology of salivary gland tumors is diverse. The classification system of the World Health Organization (WHO) contains at least 24 histopathological types of salivary gland carcinomas. The management of salivary gland carcinomas can be confusing due to the extreme diversity of tumor types, their relative rarity, the requirement for long-term follow-up, and strategy for treatment in many instances to predict outcome. Although the clinical parameters, such as clinical stage, age, and tumor location, are important for the prognostic factors in salivary gland carcinoma, histological grading also ranks highly as a critical prognostic factor. Histological grading may stratify the risk of lymph node metastasis and give a rationale for the extent of

surgery and the need for adjuvant therapy [2]. If surrogate biomarkers associated with histological grade and/or outcome could be identified, they would become powerful indicators of the optimal treatment strategy for patients with salivary gland carcinoma.

We identified actinin-4, an actin-bundling protein encoded by *ACTN4*, as a biomarker that could be used to evaluate the invasion and metastasis capabilities of cancer cells [3]. The overexpression of actinin-4 proteins was closely associated with the invasive phenotypes of some cancers, such as breast [3], colorectal [4, 5], ovarian [6, 7], bladder [8, 9], oral squamous cell [10], pancreas [11, 12], and lung carcinomas [13–15]. Oncogene amplification is often observed in aggressive malignant phenotypes of cancer [16]. Recently, it has been reported that the amplification of *ACTN4* can strictly predict the clinical outcome, and *ACTN4* has been recognized as an oncogene [6, 11, 13].

In the present study, we investigated the copy number of *ACTN4* in salivary gland carcinomas by using fluorescent in situ hybridization (FISH). Copy number increase (CNI) of *ACTN4* was positively associated with histological grade and poor outcome. We identified the biomarker to predict the outcome of salivary gland carcinoma.

This is the first report to examine the clinical usage of CNI of *ACTN4* as a prognostic factor in salivary gland carcinoma.

Patients and Methods

Patients and tissue samples

We reviewed the clinicopathological records of 58 patients who underwent surgical resection with curative intention for salivary gland carcinoma at the National Cancer Center Central Hospital (Tokyo, Japan) between 1997 and 2011.

Formalin-fixed paraffin-embedded tissue samples of 58 salivary gland carcinomas and 10 normal submandibular gland or parotid gland specimens were collected and reviewed in our institution (T. M.) according to the WHO classification of salivary gland carcinomas (Table 1). Histological grade was determined according to the three-tiered grading system proposed by Jouzdani [17].

This study was approved by the ethics committee of the National Cancer Center (approval #2010-0759).

TMA construction

Tissue microarrays (TMAs) were prepared from formalin-fixed paraffin-embedded pathological blocks, as previously described [18]. TMA blocks were cut into 4-μm-thick sections and subjected to FISH and immunohistochemistry (IHC) [4, 11].

Fluorescence in situ hybridization

The FISH probe of bacterial artificial chromosome clone containing *ACTN4* and chromosome 19p (a control clone) was purchased from Abnova (Taipei, Taiwan) [13].The labeled bacterial artificial chromosome clone DNA was subjected to FISH as previously described. TMAs were hybridized with FISH probes at 37°C for 48 h. The nuclei were counterstained with 4, 6-duamidino-2-phenylindone. The number of fluorescence signals corresponding to the copy number of *ACTN4* and control signals in the nuclei of 20 interphase tumor cells was counted (Y. W. and K. H.).

FISH patterns were defined as described previously [19, 20]. Briefly, the samples were grouped as normal disomy (two or less *ACTN4* signals in more than 90% of cells), low polysomy (four or more *ACTN4* signals in more than 10% but less than 40% of tumor cells), high polysomy (four or more *ACTN4* signals in more than 40% of tumor cells), and gene amplification (ratio *ACTN4*/chromosome more than 2, or 15 copies in more than 10% of tumor cells) [19, 20].

Immunohistochemistry

The anti-actinin-4 monoclonal antibody (13G9), which we originally established, was purchased from Transgenic Inc. (Kumamoto, Japan) [14]. Immunostaining of actinin-4 proteins was performed with the Ventana DABMap detection kit and an automated slide stainer (Discovery XT; Ventana Medical System, Tucson, AZ) [13, 14]. The expression level of actinin-4 protein was classified as: no expression (immunoreactivity score, 0), in which no tumor cells were stained with anti-actinin-4 antibody; weak expression (+1), in which tumor cells were stained with weaker intensity than endothelial cells; moderate expression (+2), in which less than 30% of tumor cells were stained; and strong expression (+3), in which more than 30% of tumor cells were stained. Two independent investigators (Y. W. and T. M.) who had no clinical information about the cases evaluated the staining patterns.

Statistical analysis

Significant differences were detected by using the Mann–Whitney *U* test, Student's *t*-test, Pearson's chi-square test, and Fisher's exact test. Overall survival was measured as the period from surgery to the date of death or last follow-up and was estimated by the Kaplan–Meier analysis. Differences between the overall survival curves were assessed with the log-rank test. Univariate and multivariate analyses were performed with the Cox regression model. Data were analyzed with the StatFlex statistical software package (version 6.0; Artiteck, Osaka,

Table 1. Association of *ACTN4* with clinicopathological characteristics of salivary gland cancer patients.

	ACTN4 FISH			Actinin-4 IHC		
	NCN	CNI	*P*-value	Negative (0, +1)	Positive (+2, +3)	*P*-value
Total	44 (75.9%)	14 (24.1%)		19 (32.8%)	39 (67.2%)	
ADCC	20 (95.2%)	1 (4.8%)		3 (14.3%)	18 (85.7%)	
CAEPA	8 (72.7%)	3 (27.3%)		5 (45.5%)	6 (54.5%)	
EMYC	2 (66.7%)	1 (33.3%)		0	3 (100%)	
MYC	0	1 (100%)		1 (100%)	0	
ACCC	3 (100%)	0		1 (33.3%)	2 (66.7%)	
ACNOS	5 (71.4%)	2 (28.6%)		4 (57.1%)	3 (42.9%)	
MEC	3 (75.0%)	1 (25.0%)		2 (50.0%)	2 (50.0%)	
SDC	2 (50.0%)	2 (50.0%)		2 (50.0%)	2 (50.0%)	
SC	1 (33.3%)	2 (66.7%)		0	3 (100%)	
OC	0	1 (100%)		1 (100%)	0	
Age						
<67 years	26 (83.9%)	5 (16.1%)	0.1267	9 (29.0%)	22 (71.0%)	0.5170
≥67 years	18 (66.7%)	9 (33.3%)		10 (37.0%)	17 (63.0%)	
Gender						
Men	24 (75.0%)	8 (25.0%)	0.8648	13 (40.6%)	19 (59.4%)	0.1567
Women	20 (76.9%)	6 (23.1%)		6 (23.1%)	20 (76.9%)	
Size						
T1–T2	12 (100%)	0	0.0503	4 (33.3%)	8 (66.7%)	1.000
T3–T4	28 (68.3%)	13 (31.7%)		14 (34.1.%)	27 (65.9%)	
Unknown	4 (80.0%)	1 (20.0%)		1 (20.0%)	4 (80.0%)	
Lymph node metastasis						
Absent	31 (79.5%)	8 (20.5%)	0.5141	10 (25.6%)	29 (74.4%)	0.0980
Present	13 (68.4%)	6 (31.6%)		9 (47.4%)	10 (52.6%)	
Histological grade						
Low, intermediate	**26 (86.7%)**	**4 (13.3%)**	**0.0465***	7 (23.3%)	23 (76.7%)	0.1134
High	**18 (64.3%)**	**10 (35.7%)**		12 (42.9%)	16 (57.1%)	
Neural invasion						
Absent	23 (76.7%)	7 (23.3%)	0.8822	11 (36.7%)	19 (63.3%)	0.5116
Present	21 (75.0%)	7 (25.0%)		8 (28.6%)	20 (71.4%)	
Vascular invasion						
Absent	**36 (83.7%)**	**7 (16.3%)**	**0.0326***	13 (29.5%)	31 (70.5%)	0.5141
Present	**8 (53.3%)**	**7 (46.7%)**		6 (42.9%)	8 (57.1%)	

FISH, fluorescent in situ hybridization; IHC, immunohistochemistry; ADCC, adenoid cystic carcinoma; CAEPA, carcinoma ex pleomorphic adenoma; EMYC, epithelial-myoepithelial carcinoma; MYC, myoepithelial carcinoma; ACCC, acinic cell carcinoma; ACNOS, adenocarcinoma, not otherwise specified; MEC, mucoepidermoid carcinoma; SDC, salivary duct carcinoma; SC, sebaceous carcinoma; OC, oncocytic carcinoma; NCN, normal copy number; CNI, copy number increase.

*$P < 0.05$. Statistically significant associations are highlighted in bold.

Japan) or the R-project (http://www.r-project.org/) [11, 13, 14].

Results

Determination of the copy number of *ACTN4* by FISH

We determined the copy number of *ACTN4* in salivary gland carcinomas by using FISH. Among the 58 tumors, 33 exhibited normal disomy (56.9%), 11 exhibited low polysomy (19.0%), 10 exhibited high polysomy (17.2%), and four exhibited gene amplification (6.9%) (Table 1). Tumors with normal disomy and low polysomy were defined as having normal copy number (NCN) of *ACTN4*, and tumors with high polysomy and gene amplification were defined as having a CNI of *ACTN4*, according to the definition of FISH analysis for epidermal growth factor receptor 1 (*EGFR*) (Fig. 1A and B). Fourteen of 58 tumors (24.1%) exhibited CNI, and 44 of 58 tumors exhibited NCN (75.9%). Histologically, the CNI was recognized in adenoid cystic carcinoma (ADCC) (4.8%, 1/21), carcinoma ex pleomorphic adenoma (CAEPA) (3/11, 27.3%), epithelial-myoepithelial carcinoma (EMYC) (1/3, 33.3%), myoepithelial carcinoma (MYC) (1/1, 100%), adenocarcinoma not otherwise

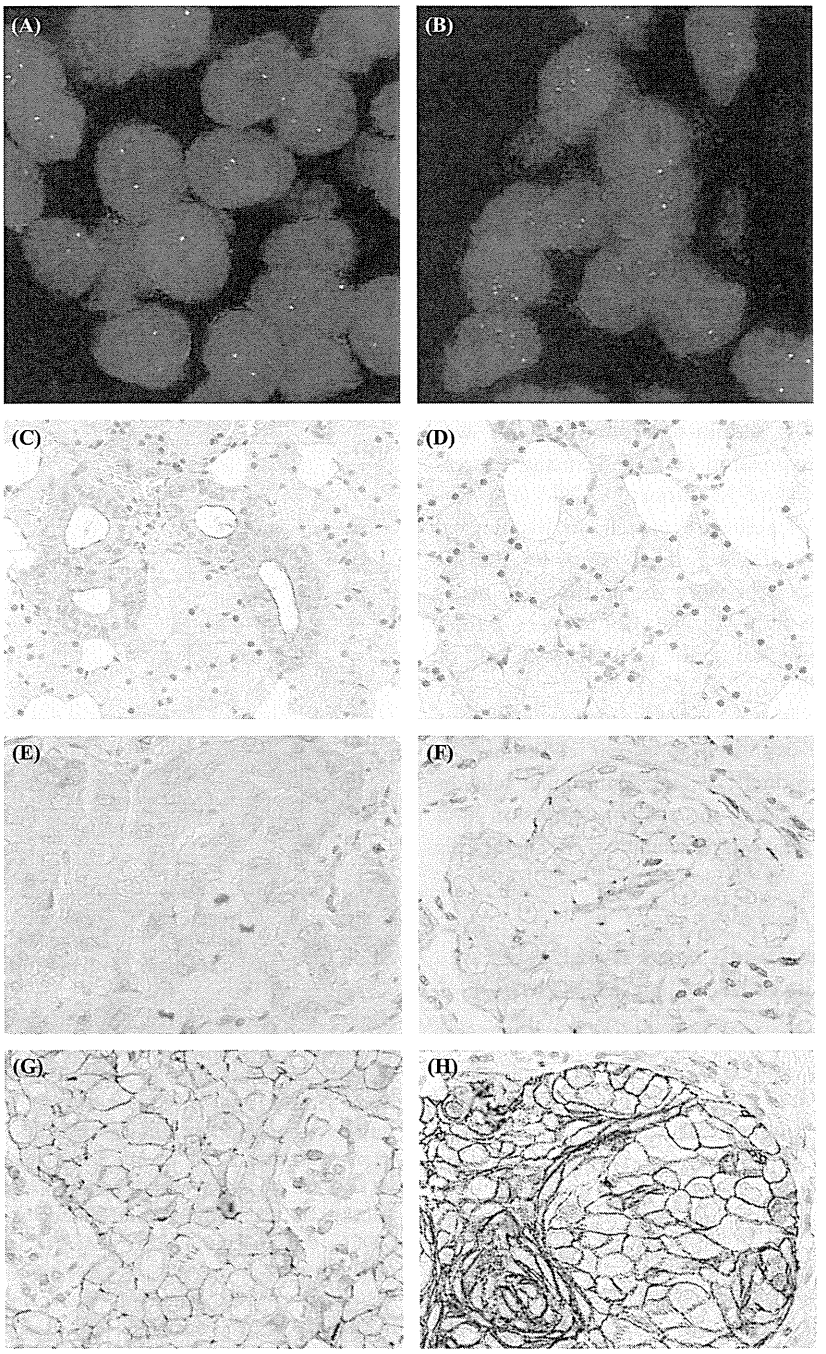

Figure 1. Representative copy number status of *ACTN4* in salivary gland cancer determined by fluorescence in situ hybridization (FISH) (A and B). Representative expression of actinin-4 protein in normal salivary gland (C and D) and salivary gland cancer (E–H), as determined by immunohistochemistry (IHC). (A) Disomy of *ACTN4* in an adenoid cystic carcinoma (ADCC), (B) gene amplification of *ACTN4* in ADCC. (C) striated duct, (D) acinar gland, (E) no expression of actinin-4 protein in mucoepidermoid carcinoma (immunoreactivities score 0), (F) weak expression, in salivary duct carcinoma (+1), (G) moderate expression in salivary duct carcinoma (+2), (H) strong expression in sebaceous carcinoma (+3).

specified (ACNOS) (2/7, 28.6%), mucoepidermoid carcinoma (MEC) (1/4, 25.0%), salivary duct carcinoma (SDC) (2/4, 50%), sebaceous carcinoma (SC) (2/3, 66.7%) and oncocytic carcinoma (OC) (1/1 100%). The NCN and CNI groups had statistically significant differences in histological grade ($P = 0.0465$) and vascular

invasion ($P = 0.0326$); however, there were no statistically significant differences in histology, age, gender, size, lymph node metastasis, or neural invasion (Table 1).

Protein expression of actinin-4 determined by IHC

We investigated the protein expression level of actinin-4 by using IHC. Among the 58 tumors, 14 (24.1%) had strong (+3) expression, 25 (43.1%) had moderate (+2) expression, 13 (22.4%) had weak (+1) expression, and six (10.3%) had no (0) expression.

Positive staining for actinin-4 protein, which was defined as moderate expression (+2) and strong expression (+3), occurred in 39 of 58 tumors (67.2%) (Fig. 1E–H). The distribution of actinin-4 protein in histological subtypes is described in Table 1. There were no statistically significant differences between the positive and negative staining groups in terms of age, gender, size, lymph node metastasis, histological grade, neural invasion, or vascular invasion (Table 1).

In normal submandibular salivary glands, actinin-4 proteins were equally expressed in acinar cells, intercalated duct cells, striated duct cells and endothelial cells. In contrast, in the parotid gland, the protein expression level of actinin-4 in acinar cells was weaker than in ductal cells (Fig. 1C and D).

The correlation between copy number of *ACTN4* and protein expression of actinin-4

We confirmed the correlation between *ACTN4* copy number and protein expression of actinin-4. CNI of *ACTN4* was recognized in 12 of 39 (30.8%) tumors with positive staining of actinin-4. CNI was recognized in six of 14 (42.9%) tumors with strong (+3) expression of actinin-4, six of 25 (24.0%) tumors with moderate (+2) expression, and two of 19 (10.5%) tumors with negative (0 and +1) staining (Fig. 2A). Although 18 of 21 ADCCs were positively stained for actinin-4 (85.7%), CNI of *ACTN4* was recognized in only one ADCC (4.8%) (Fig. 2A). Therefore, we considered that the expression level of actinin-4 protein is not positively associated with CNI of *ACTN4* in ADCC. We then investigated the correlation between protein expression levels and copy number of *ACTN4* in salivary gland carcinomas excluding ADCCs. The average copy numbers of *ACTN4* in salivary gland carcinomas excluding ADCC were 5.12, 2.90, and 2.47 in tumors with strong expression (+3), moderate expression (+2), and negative staining (0 and +1), respectively. Copy numbers of *ACTN4* were significantly increased in tumors with strong expression (+3) of actinin-4 in comparison

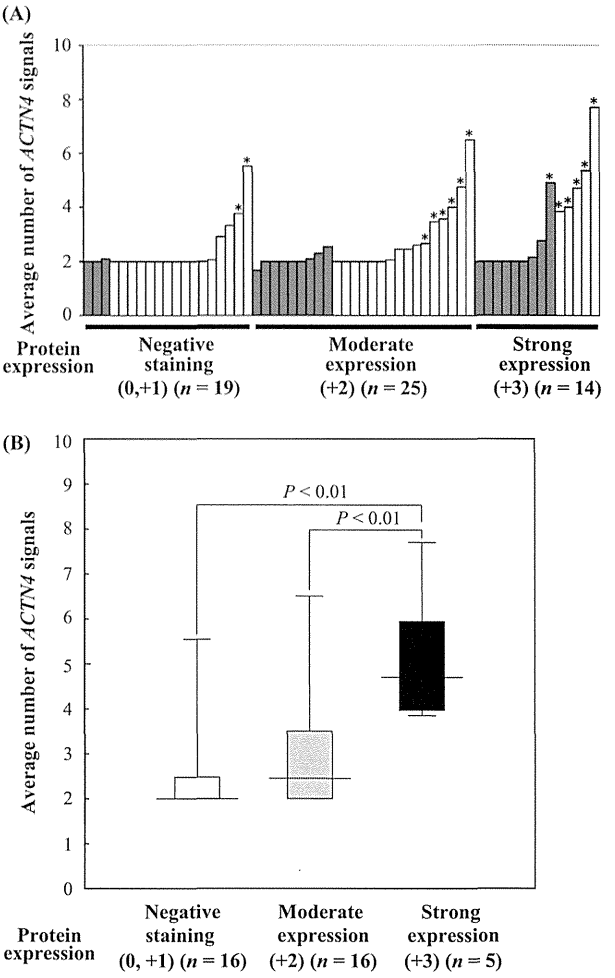

Figure 2. Collation between copy numbers of *ACTN4* and actinin-4 protein. (A) Bar graph of copy numbers of *ACTN4* in individual patients (*y*-axis; average number of *ACTN4* signals, gray bars; patients with adenoid cystic carcinoma (ADCC), white bars; patients with salivary gland carcinomas excluding ADCC, *; the patients with copy number increase [CNI]). (B) Box and whisker plot for average number of *ACTN4* signals between protein expression levels of actinin-4 proteins in the patients with salivary gland carcinomas excluding ADCC. The average number of *ACTN4* signals in the patients with strong expression of actinin-4 protein was significantly higher than the patients with moderate expression or negative staining of actinin-4 protein ($P < 0.01$, Student's *t*-test).

with negative staining (0 and +1) and moderate expression (+2) ($P < 0.01$) in salivary gland carcinomas, excluding ADCC (Fig. 2B).

The prognostic significance of CNI of *ACTN4*

Kaplan–Meier analysis revealed that CNI of *ACTN4* was significantly correlated with poor outcome in overall survival of the 58 patients with salivary gland carcinoma,